Performance of weak species in the simplest generalization of the rock-paper-scissors model to four species

P. P. Avelino,[1,2,3] B. F. de Oliveira,[4] and R. S. Trintin[4]

[1]*Instituto de Astrofísica e Ciências do Espaço, Universidade do Porto, CAUP, Rua das Estrelas, PT4150-762 Porto, Portugal*

[2]*Departamento de Física e Astronomia, Faculdade de Ciências, Universidade do Porto, Rua do Campo Alegre 687, PT4169-007 Porto, Portugal*

[3]*School of Physics and Astronomy, University of Birmingham, Birmingham B15 2TT, United Kingdom*

[4]*Departamento de Física, Universidade Estadual de Maringá, Avenida Colombo 5790, 87020-900 Maringá, PR, Brazil*

(Received 8 April 2020; accepted 4 June 2020; published 22 June 2020)

We investigate the problem of the predominance and survival of "weak" species in the context of the simplest generalization of the spatial stochastic rock-paper-scissors model to four species by considering models in which one, two, or three species have a reduced predation probability. We show, using lattice based spatial stochastic simulations with random initial conditions, that if only one of the four species has its probability reduced, then the most abundant species is the prey of the "weakest" (assuming that the simulations are large enough for coexistence to prevail). Also, among the remaining cases, we present examples in which "weak" and "strong" species have similar average abundances and others in which either of them dominates—the most abundant species being always a prey of a weak species with which it maintains a unidirectional predator-prey interaction. However, in contrast to the three-species model, we find no systematic difference in the global performance of weak and strong species, and we conjecture that a similar result will hold if the number of species is further increased. We also determine the probability of single species survival and coexistence as a function of the lattice size, discussing its dependence on initial conditions and on the change to the dynamics of the model which results from the extinction of one of the species.

DOI: 10.1103/PhysRevE.101.062312

I. INTRODUCTION

Predator-prey models are a useful tool in the study of population dynamics in biological systems (see [1–3] for the pioneer work by Lotka and Volterra, and May and Leonard). Among these, the spatial stochastic rock-paper-scissors (RPS) model describes the space-time evolution of three competing populations subject to cyclic nonhierarchical predator-prey interactions as well as reproduction and mobility. In the classical spatial stochastic RPS model [4–6], in which all the species have the same strength, the stable coexistence of all three species is generally possible if mobility is not too large. Despite its simplicity, this model is able to successfully reproduce key dynamical features observed in simple biological systems with nonhierarchical selection [4,7,8].

The classical RPS model has been generalized to include additional species and interactions [9–27]. Complex dynamical spatial structures (such as spirals with an arbitrary number of arms [13,24,28], domain interfaces with or without nontrivial internal dynamics [29], and string networks with or without junctions [30,31]), diverse scaling laws [13,22], and phase transitions [32–40] have been shown to arise naturally in many of these models. In most of them, every species has the same strength, which results in the same average density for all species (if coexistence prevails) and a survival probability mainly dependent on initial conditions (in the absence of additional biases).

In [41], it has been shown that "weak" species have a competitive advantage in the context of a Lotka-Volterra implementation of the RPS model in which one of the three species—usually refereed to as the "weakest"—has a reduced predation probability. This problem has recently been revisited in the context of Lotka-Volterra and May-Leonard formulations of the spatial stochastic RPS model with random initial conditions [42]. There, it has been shown that despite the different population dynamics and spatial patterns, these two formulations lead to qualitatively similar results for the late time values of the relative abundances of the three species, as long as the simulation lattices are sufficiently large for coexistence to prevail, the weakest species generally having an advantage over the others (especially over its predator). On the other hand, in the case of small simulation lattices, a significant dependence of the probability of species survival on the lattice size has been found, associated to the relatively large oscillations taking place at the early stages of the simulations.

Here we study the problem of the predominance and survival of weak species in the simplest generalization of the spatial stochastic RPS model to an arbitrary number of species (N_S) introduced in [13]. This model considers a modification to cyclic predator-prey models which introduces a bidirectional predation interaction of equal strength between the pairs of species for which a predator-prey interaction was absent. While in pure cyclic models parity effects have been found to be important, both in terms of the structure of the spatial patterns and of the overall dynamics [13,43,44], no significant dependence on whether the number of species is even or odd has been observed in the case of this extension of the RPS model to an arbitrary number of species. In fact,

this model has been shown to give rise to a population network characterized by spiral patterns with N_S arms, both for odd and even N_S, assuming that all the species have an equal strength. In this paper, we relax this assumption and investigate whether the positive impact of a reduced predation probability on species performance remains significant when the number of species is increased from three to four.

The outline of this paper is as follows. We start by introducing the generalization of the spatial stochastic RPS model studied in the present paper, as well as its numerical implementation, in Sec. II. In Sec. III, we present and discuss the results of a large number of spatial stochastic numerical simulations. Special emphasis is given to the way in which the average densities are affected by the reduced predation probabilities when coexistence prevails and to the dependence of the survival probability on the size of the simulation lattices. Finally, we conclude in Sec. IV.

II. SPATIAL STOCHASTIC RPS4 MODEL

In [13], it has been shown, in the context of the simplest generalization of the spatial stochastic RPS model to N_S species, that spirals with N_S arms may arise in the context of competition models. Here, we shall focus on the May-Leonard formulation of the four-species subclass of this family of models, which we shall refer to as RPS4. To this end, we shall consider a square lattice (see [45–48] for other lattice configurations) with N^2 sites and periodic boundary conditions—N shall be referred to as its linear size. The different species are labeled by i (or j), with $i, j = 1, \ldots, 4$, and modular arithmetic, where integers wrap around upon reaching 1 or 4, is assumed (the integers i and j represent the same species whenever $i = j \bmod 4$, where mod denotes the modulo operation).

In the May-Leonard formulation, every site is either empty or occupied by a single individual of one of the four species. The number of individuals of the species i and the number of empty sites will be denoted by I_i and I_0, respectively—the density of individuals of the species i and the density of empty sites shall be defined by $\rho_i = I_i/N^2$ and $\rho_0 = I_0/N^2$, respectively. The possible interactions are predation,

$$i\, j \to i\, 0,$$

reproduction,

$$i\, 0 \to i\, i,$$

and mobility,

$$i \odot \to \odot\, i,$$

where $j \neq i, i-1$ and $\odot$ represents either an individual of any species or an empty site. Reproduction and mobility interactions occur, respectively, with probabilities r and m (assumed to be the same for all the species). On the other hand, the predator-prey interactions of our baseline model are represented in Fig. 1, where the one-sided arrows represent one-directional predator-prey interactions between species i and $i+1$, while the double-sided arrows represent bidirectional predator-prey interactions between species i and $i+2$. In our baseline model, the predation probability p is the same for all species. However, in this paper, we shall investigate the dynamical impact of a reduction of the predation probability by a factor of $\mathcal{P}_w \in [0, 1]$ of one, two, or three of the four species.

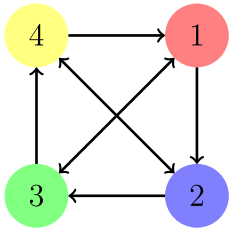

FIG. 1. Scheme of the predator-prey interactions of our baseline RPS4 model.

At every simulation step, the algorithm randomly picks an occupied site to be the active one, randomly selects one of its adjacent neighbor sites to be the passive one, and randomly chooses an interaction to be executed by the individual at the active position: Predation, mobility, or reproduction with probabilities p, m, and r, respectively—in this paper, we use the von Neumann neighborhood (or 4-neighborhood) composed of a central cell (the active one) and its four nondiagonal adjacent cells (it has been shown in [42], in the context of a three-species model, that a Moore neighborhood leads to the same qualitative results). These three actions are repeated until a possible interaction is selected—note that the interaction cannot be carried out whenever predation is selected and the passive is not a prey of the active, or if reproduction is selected and the passive is not an empty site. A generation time (our time unit) is defined as the time necessary for N^2 successive interactions to be completed.

III. RESULTS

In this section, we shall describe the results of spatial stochastic numerical simulations of the spatial RPS4 model in which one, two, or three species have a reduced predation probability—again, these species shall be referred to as weak and the others as strong.

Figures 2(a)–2(d) display the evolution of the densities of the different species and empty sites (ρ_i and ρ_0, respectively) over time for single realizations of the spatial stochastic RPS4 model (May-Leonard formulation), starting from random initial conditions with $\rho_1 = \rho_2 = \rho_3 = \rho_4 = 1/4$. The model parameters are $m = 0.2$, $p = 0.4$, $r = 0.4$, $\mathcal{P}_w = 0.5$; $p_1 = p\mathcal{P}_w$, $p_2 = p_3 = p_4 = p$ (only species 1 is weak) [Fig. 2(a)]; $p_1 = p_2 = p\mathcal{P}_w$, $p_3 = p_4 = p$ (species 1 and 2 are weak) [Fig. 2(b)]; $p_1 = p_3 = p\mathcal{P}_w$, $p_2 = p_4 = p$ (species 1 and 3 are weak) [Fig. 2(c)]; $p_1 = p_2 = p_3 = p\mathcal{P}_w$, $p_4 = p$ (species 1, 2, and 3 are weak) [Fig. 2(d)], with the strong and weak species being represented, respectively, by a filled circle and a circumference. The lower panels of each graph show snapshots of the spatial distribution of the different species on a 1000^2 lattice at $t_0 = 0$, $t_1 = 50$, $t_2 = 100$, $t_3 = 150$, $t_4 = 200$, $t_5 = 250$, $t_6 = 750$, and $t_7 = 5000$. Species 1, 2, 3, and 4 are represented in red, blue, green, and yellow, respectively, while the empty sites are left in white. Notice the changes in the background color at the early stages of simulations associated to rapid changes in the densities of the four species

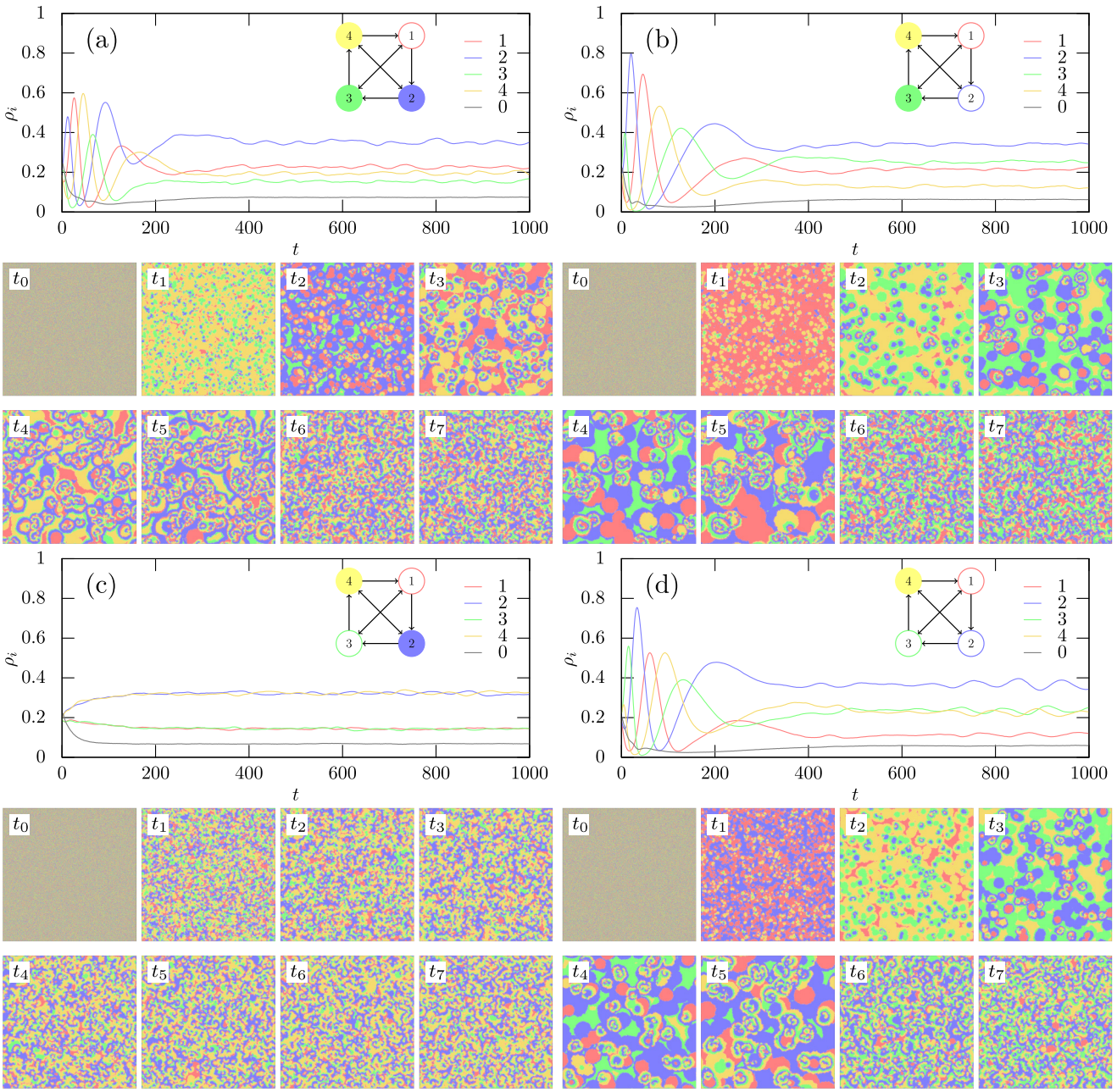

FIG. 2. (a)–(d) The evolution of the densities of the different species and empty sites (ρ_i and ρ_0, respectively) over time for single realizations of the spatial stochastic RPS4 model (May-Leonard formulation), starting from random initial conditions with $\rho_1 = \rho_2 = \rho_3 = \rho_4 = 1/4$. The model parameters are $m = 0.2$, $p = r = 0.4$, $\mathcal{P}_w = 0.5$. The strong and weak species are represented, respectively, by a filled circle and a circumference. The lower panels of each graph show snapshots of the spatial distribution of the different species on a 1000^2 lattice at $t_0 = 0$, $t_1 = 50$, $t_2 = 100$, $t_3 = 150$, $t_4 = 200$, $t_5 = 250$, $t_6 = 750$, and $t_7 = 5000$. Notice the changes in the background color at the early stages of simulations associated to rapid changes in the densities of the four species observed in graphs (a), (b), and (d).

observed in Figs. 2(a), 2(b), and 2(d), before the steady-state configuration characterized by a distinctive spatial pattern consisting of a network of four-armed spirals is attained.

Figure 2 shows two cases [Figs. 2(b) and 2(d)] in which one of the weak species is the most abundant and another two [Figs. 2(a) and 2(c)] in which that does not happen. The two cases where there is a significant difference in the average abundance of weak and strong species are the case shown in Fig. 2(b), in which one of the weak species is the most abundant, and the case shown in Fig. 2(c), in which there is a significant advantage for both strong species. Nevertheless, Fig. 2 already suggests that the average performance of weak and strong species is, in general, not very different if the simulations are sufficiently large for coexistence to prevail. Notice that in the case shown in Fig. 2(c), due to the model symmetry, the performance of the two weak species is identical (the same holding for the two strong species).

In order to investigate this aspect further, we performed a large number of simulations of the cases shown in Figs. 2(a)–2(d) with $m = 0.2$, and $p = r = 0.4$, but variable $\mathcal{P}_w$.

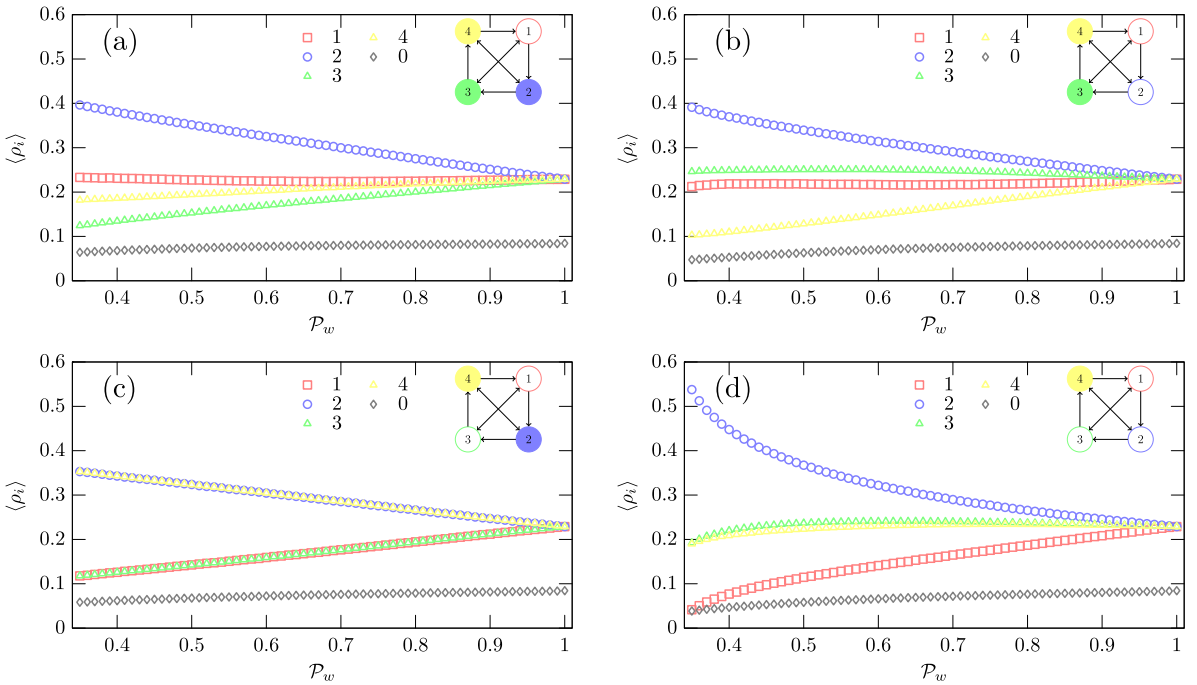

FIG. 3. Average densities of the various species as a function of $\mathcal{P}_w$ assuming $m = 0.2$, $p = r = 0.4$. Each point results from an average over the last 10^4 generations of 2000^2 simulations with a time span equal to 1.5×10^4 generations. Notice that in cases (a) and (c), the most abundant species is strong, while in cases (b) and (d), the most abundant species is weak. Also, the most abundant species in all cases (the blue species) is always a prey of a weak species with which it maintains a unidirectional predator-prey interaction.

Figure 3 shows the value of the average density of the four species as a function of $\mathcal{P}_w$. The data points result from an average over the last 10^4 generations of simulations with a time span equal to 1.5×10^4 generations performed on a 2000^2 lattice, large enough to guarantee the preservation of coexistence in all simulations. The results for $\mathcal{P}_w = 1$ were computed first, starting from random initial conditions. The final conditions of the simulations with $\mathcal{P}_w = 1$ were then taken as initial conditions of new simulations with $\mathcal{P}_w = 1$–0.01. The same procedure was repeated until $\mathcal{P}_w = 0.35$ was reached, thus ensuring a fast convergence of the simulations for every value of $\mathcal{P}_w$.

Figure 3 shows that the most abundant species is strong in the cases shown in Figs. 3(a) and 3(c), and weak in the cases shown in Figs. 3(b) and 3(d). Again, note that due to the model symmetry, and except for the different labeling, the two strong and the two weak species in the case shown in Fig. 3(c) are indistinguishable. In order to verify whether the species strength, on its own, is an advantage or disadvantage in terms of the overall abundance, we define the average density of weak and strong species as

$$\langle \rho_w \rangle = \frac{1}{\#W} \sum_{i \in W} \langle \rho_i \rangle, \quad \langle \rho_s \rangle = \frac{1}{\#S} \sum_{i \in W} \langle \rho_i \rangle, \tag{1}$$

where W and S are, respectively, the sets whose elements are the weak and strong species, and # is used to represent the number of elements of each set. Let us also define the parameter

$$\mathcal{A}_w = \frac{\langle \rho_w \rangle - \langle \rho_s \rangle}{\max(\langle \rho_w \rangle, \langle \rho_s \rangle)}, \tag{2}$$

whose absolute value represents the relative advantage (if $\mathcal{A}_w > 0$) or disadvantage (if $\mathcal{A}_w < 0$) in being a weak species. Figure 4 shows the value of $\mathcal{A}_w$ as a function of $\mathcal{P}_w$ for the cases shown in Figs. 3(a)–3(d). It shows a case [case (a)] in which there is, on average, no advantage or disadvantage in being the weakest species, another [case (c)] in which the weak species have a significant disadvantage over the others, and another two in which the weak species have some advantage over the strong species [case (d), especially for $\mathcal{P}_w \lesssim 0.5$, and case (b)]. Globally, these results show that the average performance of weak and strong species is not significantly different. Hence, we may conclude that the predominance of the weak species observed in RPS models with three species

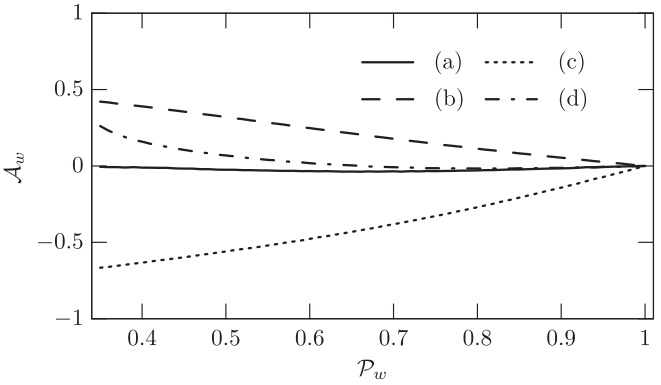

FIG. 4. The relative advantage in being a weak species $\mathcal{A}_w$ (or disadvantage if $A_w < 0$) as a function of $\mathcal{P}_w$ for the cases (a)–(d) considered in Figs. 2 and 3. Although the performance of weak and strong species varies from case to case, their global average performance is not significantly different.

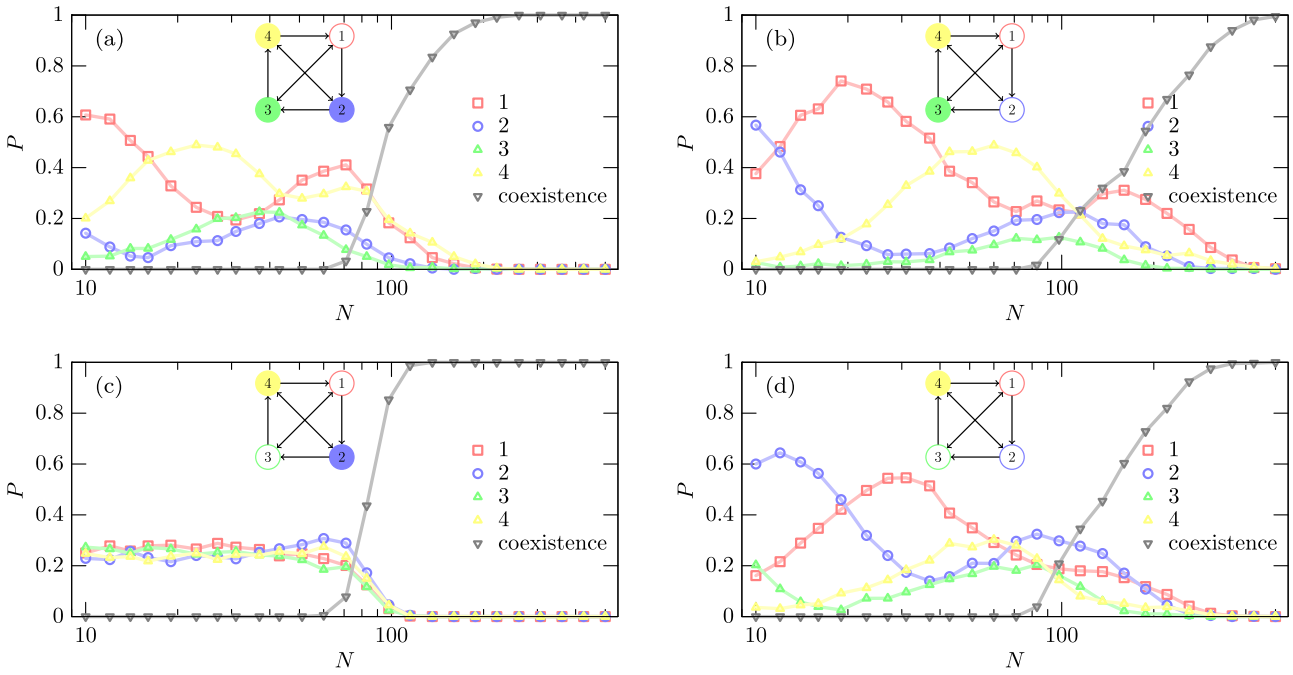

FIG. 5. Probability P of single species survival and coexistence as a function of the linear lattice size N assuming the same parameters considered in Fig. 2. Each point was estimated from 10^3 simulations with a total simulation time equal to 2×10^4 generations, starting from random initial conditions with $\rho_1 = \rho_2 = \rho_3 = \rho_4 = 1/4$. The error bars are always smaller than the size of the symbols.

no longer holds when the number of species is increased to four, and we conjecture that a similar result will hold if the number of species is further increased. Nevertheless, parity effects may play a role, especially for low values of N_S, which we plan to investigate in future work.

Figure 5 displays the probability P of single species survival and coexistence as a function of the linear lattice size N for a May-Leonard formulation of the spatial stochastic RPS4 model with $m = 0.2$, $p = 0.4$, $r = 0.4$, $\mathcal{P}_w = 0.5$; and $p_1 = p\mathcal{P}_w$, $p_2 = p_3 = p_4 = p$ [Fig. 5(a)]; $p_1 = p_2 = p\mathcal{P}_w$, $p_3 = p_4 = p$ [Fig. 5(b)]; $p_1 = p_3 = p\mathcal{P}_w$, $p_2 = p_4 = p$ [Fig. 5(c)]; and $p_1 = p_2 = p_3 = p\mathcal{P}_w$, $p_4 = p$ [Fig. 5(d)]. Each point was estimated from 10^3 simulations with a total simulation time equal to 2×10^4 generations, starting from random initial conditions with $\rho_1 = \rho_2 = \rho_3 = \rho_4 = 1/4$. The error bars are always smaller than the size of the symbols, with the one-sigma uncertainty in the value of P at each point being approximately equal to $[P(1-P)/10^3]^{1/2}$, with a maximum of approximately 1.6×10^{-2} for $P = 0.5$.

Figure 5 shows that the transient coherent oscillations of the abundances of the four species in the early stages of simulations [Figs. 2(a), 2(b), and 2(d)] are responsible for a significant dependence of the survival probability on the linear size of the lattices—a feature also observed in the context of a three-species RPS model in which one of the species has a reduced predation probability [42]. Also, it is interesting to note that the species with the largest survival probability is not necessarily the most abundant species in Fig. 3, even if the probability of coexistence is high. In fact, in the cases shown by Figs. 3(b) and 3(d), the red species is only the third and fourth most abundant, respectively, as long as the linear size of the simulations is large enough for coexistence to prevail. However, for $N_{th} > 100$ and $N_{th} > 200$, respectively, the red species is the one with the highest survival probability in Figs. 5(b) and 5(d). The explanation of this apparent inconsistency resides in the fact that once one of the species disappears, there is a significant change in the nature of the model.

In fact, above a given linear size threshold, the first species to become extinct is typically the least abundant in Fig. 3. Once that happens, the remaining species may then be classified as a function of a strength parameter S_k, with the subscript $k = -1, 0$, or 1 representing the number of preys minus the number of predators ($S_{-1} = i + 3$, $S_0 = i + 2$, and $S_1 = i + 1$, where i is the species that is the first to become extinct). We verified that, in general, once species i vanishes, species $S_{-1} = i + 3$ and $S_0 = i + 2$ also become extinct (in that order), with the species $S_1 = i + 1$ (the prey of the first species to become extinct) being the one surviving in the end.

This correspondence between the first species to become extinct and the surviving species may be confirmed by comparing Figs. 5 and 6—Fig. 6 displays the probability P^* that the species i is the first species to become extinct, or that the coexistence of the four species is maintained, as a function of the linear lattice size N for the same simulations considered in Fig. 5. Again, the error bars are always smaller than the size of the symbols, with the one-sigma uncertainty in the value of P^* at each point being approximately equal to $[P^*(1-P^*)/10^3]^{1/2}$, with a maximum of approximately 1.6×10^{-2} for $P^* = 0.5$. Under the transformation $i \to i + 1$, Fig. 6 would become very similar to Fig. 5, thus confirming our analysis. For example, in the case shown by Fig. 5(b), if the coexistence probability is high, one would expect that species 4 [yellow: The least abundant species shown in Fig. 3(b)] would be the one with the higher extinction probability [this may be confirmed in Fig. 6(b) for $N > 100$], thus implying

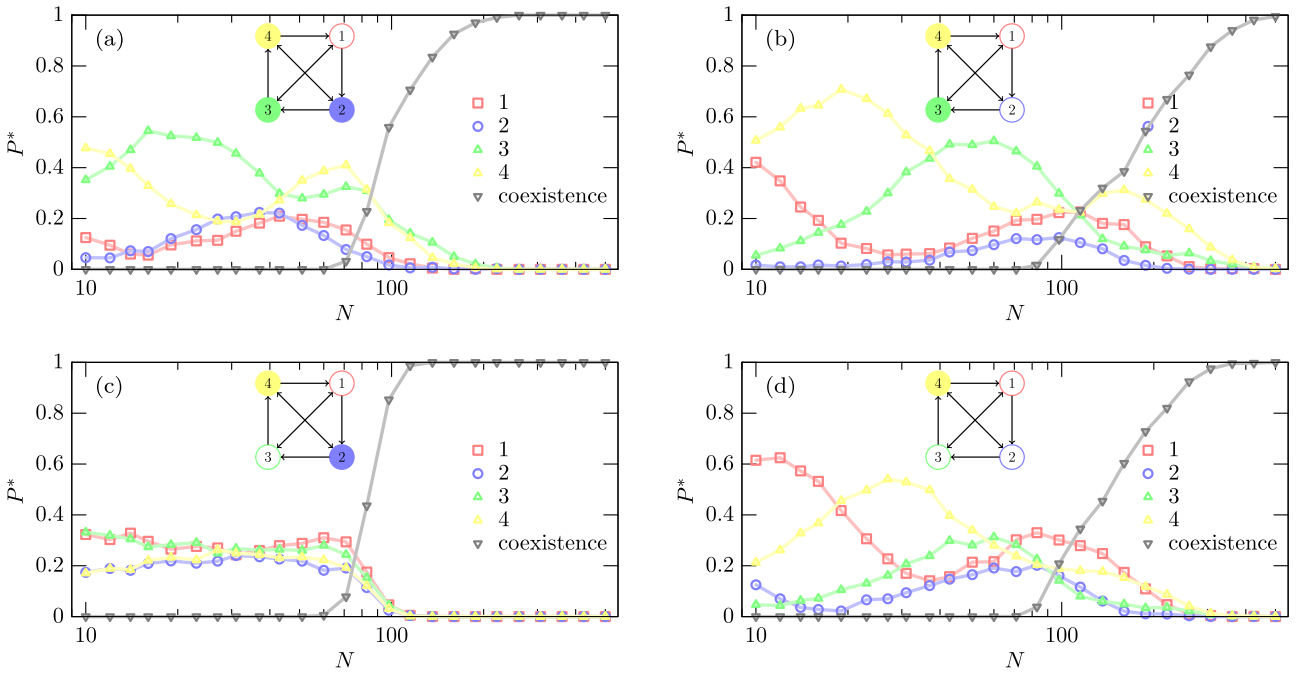

FIG. 6. Probability P^* that the species i is the first species to become extinct, or that the coexistence of the four species is maintained, as a function of the linear lattice size N. P^* was estimated using the same simulations considered in Fig. 5.

that its prey (red species 1) should be the one with the highest survival probability [this may be confirmed in Fig. 5(b) for $N > 100$].

We have also considered a modification of our model where there is no reduction to predation probabilities between species with bidirectional predator-prey interactions, and verified that this change has no significant impact on our results.

IV. CONCLUSIONS

In this paper, we have added a dimension to the problem of the predominance and survival of weak species by investigating the simplest generalization of the spatial stochastic RPS model to four species in which one or more species has a reduced predation probability. We have shown, using lattice based spatial stochastic simulations of a May-Leonard model formulation, that if only one of the four species has a reduced predation probability, it is the prey of the weakest that is the most abundant species, as long as the simulations are large enough for coexistence to be maintained. This is in contrast with the three-species model where the weakest species is generally the most abundant. By considering cases with more than one weak species, we have also found that unlike in the case of the three-species model, there is no significant average advantage or disadvantage associated to being "weak" or "strong". We have also shown that in the RPS4 model, once one of the species becomes extinct, the surviving species is typically its prey, this result being largely independent of the number of weak and strong species and of the specific value of the parameter characterizing the reduction of the predation probability of the weak species.

Our results are consistent with those obtained in [6], where the basins of attraction for species extinction and coexistence have been investigated in the case of the standard spatial RPS model with three species. In [6], it has been shown that the coexistence basin, consisting of the set of initial conditions which generate a final state in which all species survive and coexist, shrinks as m/N is enhanced and vanishes above a critical threshold value of m/N. On the other hand, outside the coexistence basin, which species survives has been found to be strongly dependent on initial conditions. In the present paper, we have confirmed that for a fixed m, the fact that the coexistence basin increases with N also holds in the context of a four-species generalization of the standard spatial RPS model even if one, two, or three of the species have a reduced predation probability. Furthermore, we have characterized the dependence of the late time average density of the various species in the limit of large N as a function of the reduced predation probability parameter $\mathcal{P}_w$ (in the case studied in [6], all the species had the same strength and, therefore, the same asymptotic average density inside the coexistence basin). Furthermore, the strong dependence of the surviving species on initial conditions outside the coexistence basin found in [6] is perfectly consistent with the findings of the present paper: The relatively large oscillations at the initial stages of simulations with random initial conditions are responsible for the strong dependence of the species survival probability on the lattice size.

ACKNOWLEDGMENTS

P.P.A. acknowledges the support from Fundação para a Ciência e a Tecnologia (FCT) through the Sabbatical Grant No. SFRH/BSAB/150322/2019 and through the Research Grants No. UID/FIS/04434/2019, No. UIDB/04434/2020, and No. UIDP/04434/2020. B.F.O. and R.S.T. thank CAPES - Finance Code 001, Fundação Araucária, and INCT-FCx (CNPq/FAPESP) for financial and computational support.

[1] A. J. Lotka, Proc. Natl. Acad. Sci. USA **6**, 410 (1920).
[2] V. Volterra, Nature (London) **118**, 558 (1926).
[3] R. May and W. Leonard, SIAM J. Appl. Math. **29**, 243 (1975).
[4] B. Kerr, M. A. Riley, M. W. Feldman, and B. J. M. Bohannan, Nature (London) **418**, 171 (2002).
[5] T. Reichenbach, M. Mobilia, and E. Frey, Nature (London) **448**, 1046 (2007).
[6] H. Shi, W.-X. Wang, R. Yang, and Y.-C. Lai, Phys. Rev. E **81**, 030901(R) (2010).
[7] B. Sinervo and C. M. Lively, Nature (London) **380**, 240 (1996).
[8] B. C. Kirkup and M. A. Riley, Nature (London) **428**, 412 (2004).
[9] M. Peltomäki and M. Alava, Phys. Rev. E **78**, 031906 (2008).
[10] G. Szabó, A. Szolnoki, and I. Borsos, Phys. Rev. E **77**, 041919 (2008).
[11] S. Allesina and J. M. Levine, Proc. Natl. Acad. Sci. USA **108**, 5638 (2011).
[12] P. P. Avelino, D. Bazeia, L. Losano, and J. Menezes, Phys. Rev. E **86**, 031119 (2012).
[13] P. P. Avelino, D. Bazeia, L. Losano, J. Menezes, and B. F. Oliveira, Phys. Rev. E **86**, 036112 (2012).
[14] Y. Li, L. Dong, and G. Yang, Physica A: Stat. Mech. Appl. **391**, 125 (2012).
[15] A. Roman, D. Konrad, and M. Pleimling, J. Stat. Mech.: Theory Exp. (2012) P07014.
[16] A. F. Lütz, S. Risau-Gusman, and J. J. Arenzon, J. Theor. Biol. **317**, 286 (2013).
[17] A. Roman, D. Dasgupta, and M. Pleimling, Phys. Rev. E **87**, 032148 (2013).
[18] H. Cheng, N. Yao, Z.-G. Huang, J. Park, Y. Do, and Y.-C. Lai, Sci. Rep. **4**, 7486 (2014).
[19] A. Szolnoki, M. Mobilia, L.-L. Jiang, B. Szczesny, A. M. Rucklidge, and M. Perc, J. R. Soc., Interface **11**, 20140735 (2014).
[20] Y. Kang, Q. Pan, X. Wang, and M. He, Entropy **18**, 284 (2016).
[21] A. Roman, D. Dasgupta, and M. Pleimling, J. Theor. Biol. **403**, 10 (2016).
[22] B. L. Brown and M. Pleimling, Phys. Rev. E **96**, 012147 (2017).
[23] J. Park, Y. Do, B. Jang, and Y.-C. Lai, Sci. Rep. **7**, 7465 (2017).
[24] D. Bazeia, J. Menezes, B. F. de Oliveira, and J. G. G. S. Ramos, Europhys. Lett. **119**, 58003 (2017).
[25] C. A. Souza-Filho, D. Bazeia, and J. G. G. S. Ramos, Phys. Rev. E **95**, 062411 (2017).
[26] S. Esmaeili, B. L. Brown, and M. Pleimling, Phys. Rev. E **98**, 062105 (2018).
[27] P. P. Avelino, J. Menezes, B. F. de Oliveira, and T. A. Pereira, Phys. Rev. E **99**, 052310 (2019).
[28] D. Bazeia, B. F. de Oliveira, and A. Szolnoki, Phys. Rev. E **99**, 052408 (2019).
[29] P. P. Avelino, D. Bazeia, L. Losano, J. Menezes, and B. F. de Oliveira, Phys. Rev. E **89**, 042710 (2014).
[30] P. P. Avelino, D. Bazeia, J. Menezes, and B. F. de Oliveira, Phys. Lett. A **378**, 393 (2014).
[31] P. P. Avelino, D. Bazeia, L. Losano, J. Menezes, and B. F. de Oliveira, Phys. Lett. A **381**, 1014 (2017).
[32] G. Szabó and T. Czárán, Phys. Rev. E **63**, 061904 (2001).
[33] G. Szabó and G. A. Sznaider, Phys. Rev. E **69**, 031911 (2004).
[34] A. Szolnoki and G. Szabó, Phys. Rev. E **70**, 037102 (2004).
[35] M. Perc, A. Szolnoki, and G. Szabó, Phys. Rev. E **75**, 052102 (2007).
[36] G. Szabó, A. Szolnoki, and G. A. Sznaider, Phys. Rev. E **76**, 051921 (2007).
[37] G. Szabó and A. Szolnoki, Phys. Rev. E **77**, 011906 (2008).
[38] A. Szolnoki, G. Szabó, and L. Czakó, Phys. Rev. E **84**, 046106 (2011).
[39] J. Vukov, A. Szolnoki, and G. Szabó, Phys. Rev. E **88**, 022123 (2013).
[40] D. Bazeia, B. F. de Oliveira, and A. Szolnoki, Europhys. Lett. **124**, 68001 (2018).
[41] M. Frean and E. R. Abraham, Proc. R. Soc. London B **268**, 1323 (2001).
[42] P. P. Avelino, B. F. de Oliveira, and R. S. Trintin, Phys. Rev. E **100**, 042209 (2019).
[43] K. Kobayashi and K.-i. Tainaka, J. Phys. Soc. Jpn. **66**, 38 (1997).
[44] Y. N. Sato, Kazunori and N. Konno, Appl. Math. Comput. **126**, 255 (2002).
[45] G. Szabó, A. Szolnoki, and R. Izsák, J. Phys. A: Math. Gen. **37**, 2599 (2004).
[46] G.-Y. Zhang, Y. Chen, W.-K. Qi, and S.-M. Qing, Phys. Rev. E **79**, 062901 (2009).
[47] R. A. Laird, Oikos **123**, 472 (2014).
[48] C. Rulquin and J. J. Arenzon, Phys. Rev. E **89**, 032133 (2014).